07.2

Electrical conductive and photoelectrical properties of heterostructures based on gallium and chromium oxides with corundum structure

© D.A. Almaev[1], A.V. Almaev[1,2], V.V. Kopyev[1], V.I. Nikolaev[3,4], A.I. Pechnikov[3], S.I. Stepanov[3], M.E. Boyko[3], P.N. Butenko[1,3], M.P. Scheglov[3]

[1] Tomsk State University, Tomsk, Russia
[2] Fokon LLC, Kaluga, Russia
[3] Ioffe Institute, St. Petersburg, Russia
[4] Perfect Crystals LLC, Saint-Petersburg, Russia
E-mail: almaev001@mail.ru

Received July 25, 2022
Revised September 28, 2022
Accepted September 29, 2022

α-Ga_2O_3/α-Cr_2O_3 heterostructures with a corundum structure were obtained by chloride vapor phase epitaxy and magnetron sputtering. The structural, electrical conductive and photoelectrical properties of the obtained samples were studied. It was established that the α-Ga_2O_3/α-Cr_2O_3 heterostructures exhibits weak rectifying properties and in comparison with α-Ga_2O_3 films has a higher response speed when exposed to ultraviolet radiation

Keywords: Gallium oxide, chromium oxide, corundum, anisotypic heterostructures

DOI: 10.21883/TPL.2022.11.54893.19322

Gallium oxide Ga_2O_3 is an ultra-wide-gap semiconductor that has potential for application in the design of power electronics, ultraviolet (UV) optoelectronics, and sensorics devices [1–6]. This potential is limited by certain features of the energy spectrum of Ga_2O_3 and strong localization of holes at oxygen atoms, which make a practically relevant hole conductivity unattainable [7–9]. Electron–hole junctions may be produced based on anisotype heterojunctions between Ga_2O_3 and other oxides. The α-Ga_2O_3 polymorphic form with a corundum lattice is the most promising one in terms of heterojunction formation. This crystalline modification is characterized by lattice constants $a = 0.4983$ nm and $c = 1.3433$ nm, a small effective electron mass $m_n^* \approx 0.25m_0$ (m_0 is the rest mass of an electron), and high values of the theoretical critical electric field (9 MV/cm) and bandgap width $E_g = 5.1-5.6$ eV [2,3,5–11].

The crystal structure of corundum with similar lattice parameters is typical of a large number of oxides of transition and nontransition metals with general formula M_2O_3 (M = Al, Ga, In, Fe, Cr, V, Ti, Rh, Ir) [1,5,7–9]. Chromium oxide α-Cr_2O_3 is the best-fit material for an anisotype heterojunction with α-Ga_2O_3. The lattice mismatch of α-Ga_2O_3 and α-Cr_2O_3 does not exceed 1%. This semiconductor with $E_g = 2.9-3.4$ eV features intrinsic hole conductivity and is being studied extensively for the purpose of development of transparent conductive oxides, gas sensors, and photodetectors [12–14]. α-Ga_2O_3/α-Cr_2O_3 structures may hold promise for the design of power devices and photodiodes.

The present study is focused on the examination of structural, conductive, and photoelectrical properties of anisotype α-Ga_2O_3/α-Cr_2O_3 heterojunctions.

Films of α-Ga_2O_3 with a thickness of 2 μm were grown at OOO „Sovershennye Kristally" by chloride vapor phase epitaxy with gallium chloride and oxygen gases used as precursors. The process was performed on sapphire substrates with a basal orientation at temperature $T = 500^\circ$C within 30 min. In the course of growth, α-Ga_2O_3 was doped with tin.

Thin α-Cr_2O_3 films with a thickness of 150 nm, which were produced by radio-frequency magnetron sputtering (RFMS) of a chromium target in $O_2 + Ar$ plasma, were deposited on top of epitaxial α-Ga_2O_3 layers or a sapphire substrate. An Edwards A-500 setup was used for RFMS. The operating pressure, the power, and the concentration of oxygen in the $O_2 + Ar$ were 7 μbar, 70 W, and 56.1 ± 0.5 vol.%, respectively. Sputtered α-Cr_2O_3 films were annealed in air at $T = 500^\circ$C for 180 min. Contacts with a thickness of 100 nm and an area of 0.5 mm^2 were formed on the surface of α-Ga_2O_3 and α-Cr_2O_3 films and α-Ga_2O_3/α-Cr_2O_3 structures by DC magnetron sputtering of a Ti target carried out using the same Edwards A-500 setup. In the process of Ti sputtering, masks on the surface of heterostructures were positioned so as to form contacts to each layer.

The phase composition of samples was examined by X-ray diffraction (XRD). A „DRON 6" („Burevestnik") diffractometer with CuK_α radiation ($\lambda = 1.5406$ Å) in the standard $\theta-2\theta$ configuration was used for the purpose. The surface microrelief of thin films of chromium oxide was studied with a Silver HV (NT-MDT) atomic force microscope (AFM). The transmission spectra of films at wavelengths $\lambda = 200-800$ nm were measured using Ocean Optics USB 2000+ and Ocean Insight FLAME fiber-optic spectrometers. Current–voltage curves (CVCs),

capacitance–voltage curves, and the frequency dependence of capacitance of the samples were measured using a sealed microprobe setup, a Keithley 2636A sourcemeter, and an Agilent E-4980-A RLC meter under darkroom conditions and under the influence of radiation with $\lambda = 254$ nm. A krypton–fluorine lamp with the corresponding filter served as a source of monochromatic radiation. The radiation power density was 1.3 mW/cm^2. Photocurrent density J_{ph}, current monochromatic sensitivity R^*, specific detectivity D^*, and external quantum efficiency EQE were estimated in accordance with the formulae presented in [7,9]. Twelve samples of α-Ga_2O_3/α-Cr_2O_3 structures were prepared for the examination of their electrophysical properties.

XRD spectra revealed the dominance of peaks at $2\theta = 40.9$, $87.7°$ for gallium oxide films and at $2\theta = 39.7$, $85.9°$ for thin films of chromium oxide. These peaks correspond to reflections (0006) and (00012) of α-Ga_2O_3 and α-Cr_2O_3 phases (Figs. 1, *a* and *b*, respectively). Both peaks of gallium oxide were found in the spectra of α-Ga_2O_3/α-Cr_2O_3 heterostructures and had an elevated (relative to the substrate peaks) intensity (Fig. 1, *c*). The chromium oxide peak at $2\theta = 39.7°$ did not reveal itself in the spectra of heterostructures, but the intensity of the peak at $2\theta = 85.9°$ was also elevated relative to the substrate peaks. The positions of substrate peaks were the same in all spectra. AFM studied showed that the surface of non-annealed thin α-Cr_2O_3 films was solid and remained relatively smooth throughout the entire sample area. The fine-grain structure revealed itself after annealing, which stimulated recrystallization. The mean crystallite size was 34 nm. Crystallites were oriented perpendicular to the substrate.

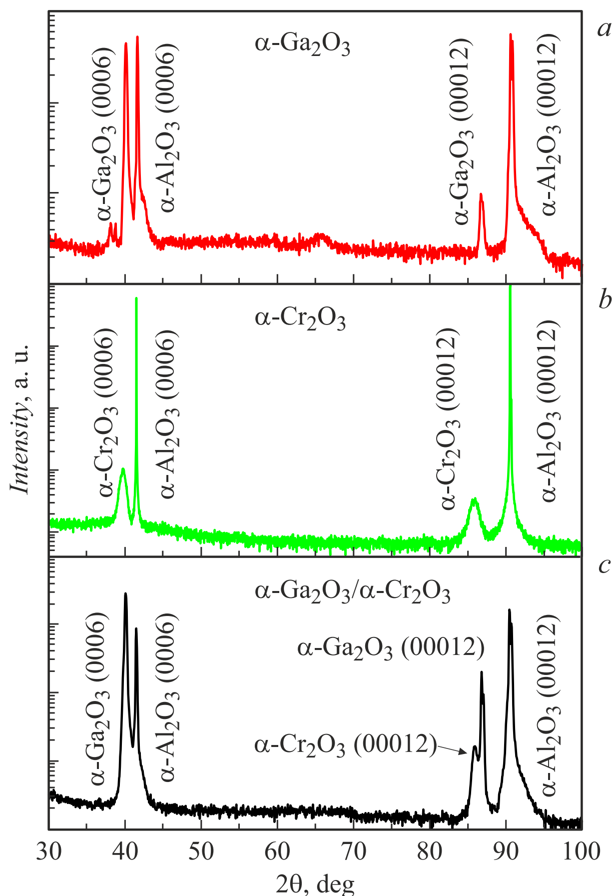

Figure 1. XRD spectra of films of gallium oxide (*a*), chromium oxide (*b*), and α-Ga_2O_3/α-Cr_2O_3 (*c*) on sapphire substrates.

The transmission coefficients were no lower than 70 and 80% at $\lambda = 550-800$ nm for α-Cr_2O_3 and $\lambda = 260-360$ nm for α-Ga_2O_3, respectively. The values of these coefficients dropped sharply as λ decreased from 400 to 320 nm for α-Cr_2O_3 films or from 260 to 240 nm for α-Ga_2O_3 films (i.e., in the vicinity of the optical self-absorption edge in these materials). Having analyzed the optical transmission spectra, we found that the obtained films are characterized by direct optical transitions; the optical bandgap width was estimated at $E_g^{opt} = 3.1 \pm 0.1$ eV for α-Cr_2O_3 and 5.1 ± 0.1 eV for α-Ga_2O_3.

Ti contacts to α-Cr_2O_3 and α-Ga_2O_3 films were Ohmic in nature and were found to be stable within the range of $T = 300-673$ K. It was established that α-Ga_2O_3 films are characterized by extremely low values of dark current density J_D at room temperature and fine photoelectrical parameters J_{ph}, J_{ph}/J_D, R^*, D^*, and EQE (see the table), which are comparable or superior to the results reported in other studies [1,4–7,14]. Rise τ_1 and fall τ_2 photoresponse times determined at the levels of $0.9J_L$ (J_L is the net electric current in a film under UV irradiation) and $1.1J_D$, respectively, were 0.1 and ~ 60 s for α-Ga_2O_3 films. High values of τ_2 are likely attributable to deep trap centers with different activation energies that, according to [15], are present in the bandgap.

The conductivity type of α-Cr_2O_3 films was determined based on the temperature dependence of the Seebeck coefficient, which was positive and grew from 41 to 86 μV/K as T increased from 373 to 573 K. These films are characterized by a higher electric conductivity than α-Ga_2O_3, but are only weakly sensitive to UV irradiation. The latter is likely associated with an enhancement of surface recombination at small λ values.

The obtained α-Ga_2O_3/α-Cr_2O_3 heterostructures exhibited weak rectifying properties (Fig. 2, *a*). The forward/backward current ratio at voltage $U = 60$ V was 71. After five cycles of UV irradiation with subsequent heating from $T = 25$ to $400°$C within 15 min, a reduction in the current under forward bias and an increase in the current under backward bias with subsequent stabilization were observed (Fig. 2, *b*). This ageing is likely associated with a change in the microstructure of α-Cr_2O_3 [16]. No further changes in CVCs were observed after 7–30 days of storage in sealed packaging. The forward/backward current ratio for aged samples (Fig. 2, *c*) is ~ 30 at $U = 2$ V, drops to 3 at $U = 16$ V, and remains almost unchanged as U grows further. It should be noted that J_D varied within an order of magnitude from one sample to the other under equal experimental and storage conditions. Let us focus our attention on aged samples. The values of J_D

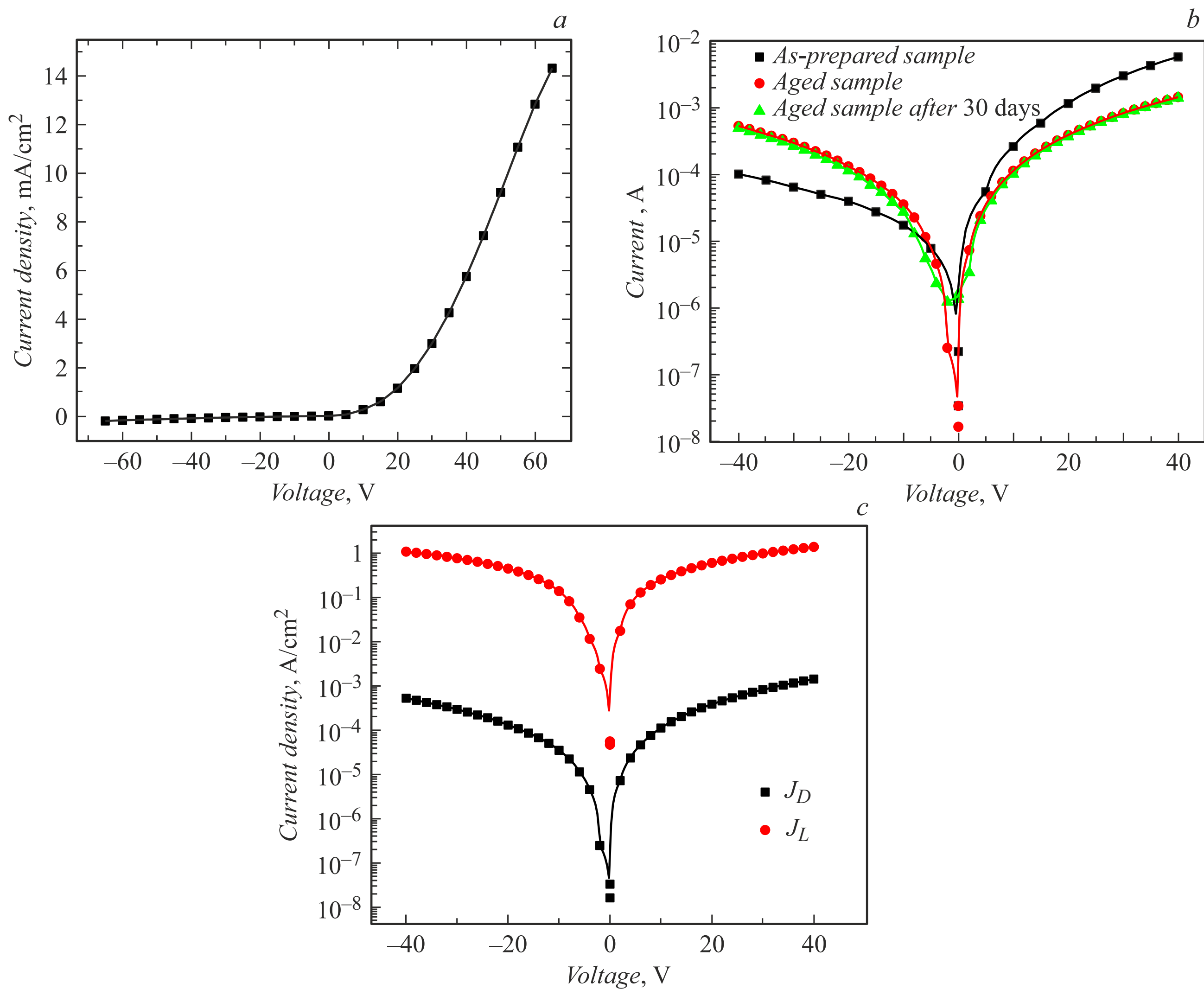

Figure 2. CVC of the α-Ga_2O_3/α-Cr_2O_3 heterostructure under darkroom conditions (*a*), evolution of the CVC of the α-Ga_2O_3/α-Cr_2O_3 heterostructure under darkroom conditions (*b*), and CVC of the aged α-Ga_2O_3/α-Cr_2O_3 heterostructure under darkroom conditions and under illumination with $\lambda = 254$ nm (*c*).

Conductive and photoelectrical properties of α-Ga_2O_3 and α-Cr_2O_3 films and α-Ga_2O_3/α-Cr_2O_3 structures at $U = 35$ V and room temperature ($T = 300$ K)

Parameter	Structure		
	α-Ga_2O_3	α-Cr_2O_3	α-Ga_2O_3/α-Cr_2O_3
J_D, nA/cm^2	420	$2.3 \cdot 10^9$	$9.8 \cdot 10^5$
J_{ph}, A/cm^2	13.9	$1.2 \cdot 10^{-2}$	1.2
J_{ph}/J_D	$3.3 \cdot 10^7$	$5.3 \cdot 10^{-3}$	$1.1 \cdot 10^3$
R^*, A/W	21.4	$6.7 \cdot 10^{-3}$	2.1
D^*, cm $\cdot$ Hz$^{1/2}$/W	$1.3 \cdot 10^{15}$	$2.9 \cdot 10^8$	$2.3 \cdot 10^{12}$
EQE, %	$1.1 \cdot 10^4$	3.3	984.5

Note. J_{ph} — photocurrent, R^* — current monochromatic sensitivity, D^* — detectivity, EQE — external quantum efficiency.

for α-Ga_2O_3/α-Cr_2O_3 under forward and backward bias are 3–4 orders of magnitude higher than J_D for α-Ga_2O_3 films. As U increases from 2 to 40 V under forward and backward bias, the value of J_D grows as a power function: $J \propto U^m$, where m is the index of power. The values of m are 1.77 ± 0.01 and 2.0 ± 0.1 for the forward and backward branches, respectively. The shape of capacitance–voltage curves and frequency dependences of capacitance of α-Ga_2O_3/α-Cr_2O_3 structures is typical of heterostructures. In our view, weak rectifying properties of α-Ga_2O_3/α-Cr_2O_3 structures are attributable, on the one hand, to the low carrier density in p-type α-Cr_2O_3 and the presence of a high density of electrically active defects in the base (i.e., n-type α-Ga_2O_3). On the other hand, the J_D increase under forward and backward bias (relative to a α-Ga_2O_3 film) is indicative of the formation of a space charge region at the interface of semiconductors. This leads to depopulation of a

fraction of trap levels in α-Ga_2O_3, and free electrons enter the conduction band of the semiconductor.

The photoelectrical parameters of α-Ga_2O_3/α-Cr_2O_3 structures are inferior to the characteristics of α-Ga_2O_3 (see the table), although τ_2 for α-Ga_2O_3/α-Cr_2O_3 is approximately 5 times shorter. This τ_2 reduction is likely attributable to the presence of an electric field, which accelerates inequilibrium electrons, in the space charge region at the interface of semiconductors.

The conductive and photoelectrical properties of anisotype heterostructures based on α-Ga_2O_3 and α-Cr_2O_3 films with a corundum structure, which were produced by chloride vapor phase epitaxy and RFMS, respectively, were studied. It was established that α-Ga_2O_3/α-Cr_2O_3 heterostructures feature weak rectifying properties and shorter (compared to α-Ga_2O_3 films) photoresponse fall times under irradiation with a wavelength of 254 nm. This is due to the formation of a space charge region with a built-in electric field at the interface of semiconductors.

Conflict of interest

The authors declare that they have no conflict of interest.

References

[1] J. Moloney, O. Tesh, M. Singh, J.W. Roberts, J.C. Jarman, L.C. Lee, T.N. Huq, J. Brister, S. Karboyan, M. Kuball, P.R. Chalker, R.A. Oliver, F.C.-P. Massabuau, J. Phys. D: Appl. Phys., **52** (47), 475101 (2019). DOI: 10.1088/1361-6463/ab3b76

[2] K. Akaiwa, K. Kaneko, K. Ichino, S. Fujita, Jpn. J. Appl. Phys., **55**, (12) 1202BA (2016). DOI: 10.7567/JJAP.55.1202BA

[3] A.K. Mondal, M.A. Mohamed, L.K. Ping, M.F.M. Taib, M.H. Samat, M.A.S.M. Haniff, R. Bahru, Materials, **14** (3), 604 (2021). DOI: 10.3390/ma14030604

[4] X.Y. Sun, X.H. Chen, J.G. Hao, Z.P. Wang, Y. Xu, H.H. Gong, Y.J. Zhang, X.X. Yu, C.D. Zhang, F.-F. Ren, S.L. Gu, R. Zhang, J.D. Ye, Appl. Phys. Lett., **119** (14), 141601 (2021). DOI: 10.1063/5.0059061

[5] X. Zhao, Z. Wu, D. Guo, W. Cui, P. Li, Y. An, L. Li, W. Tang, Semicond. Sci. Technol., **31** (6), 065010 (2016). DOI: 10.1088/0268-1242/31/6/065010

[6] D.Y. Guo, X.L. Zhao, Y.S. Zhi, W. Cui, Y.Q. Huang, Y.H. An, P.G. Li, Z.P. Wu, W.H. Tang, Mater. Lett., **164**, 364 (2015). DOI: 10.1016/j.matlet.2015.11.001

[7] X. Hou, Y. Zou, M. Ding, Y. Qin, Z. Zhang, X. Ma, P. Tan, S. Yu, X. Zhou, X. Zhao, G. Xu, H. Sun, S. Long, J. Phys. D: Appl. Phys., **54** (4), 043001 (2020). DOI: 10.1088/1361-6463/abbb45

[8] S.J. Pearton, J. Yang, P.H. Cary, F. Ren, J. Kim, M.J. Tadjer, M.A. Mastro, Appl. Phys. Rev., **5** (1), 011301 (2018). DOI: 10.1063/1.5006941

[9] D. Kaur, M. Kumar, Adv. Opt. Mater., **9** (9), 2002160 (2021). DOI: 10.1002/adom.202002160

[10] Y. Xu, C. Zhang, Y. Cheng, Z. Li, Y. Cheng, Q. Feng, D. Chen, J. Zhang, Y. Hao, Materials, **12** (22), 3670 (2019). DOI: 10.3390/ma12223670

[11] J.A. Spencer, A.L. Mock, A.G. Jacobs, M. Schubert, Y. Zhang, M.J. Tadjer, Appl. Phys. Rev., **9** (1), 011315 (2022). DOI: 10.1063/5.0078037

[12] L. Farrell, K. Fleischer, D. Caffrey, D. Mullarkey, E. Norton, I.V. Shvets, Phys. Rev. B, **91** (12), 125202 (2015). DOI: 0.1103/PhysRevB.91.125202

[13] A.V. Almaev, B.O. Kushnarev, E.V. Chernikov, V.A. Novikov, Tech. Phys. Lett., **46**, 1028 (2020). DOI: 10.1134/S106378502010017X.

[14] Z. Fan, M. Zhu, S. Pan, J. Ge, L. Hu, Ceram. Int., **47** (10A), 13655 (2021). DOI: 10.1016/j.ceramint.2021.01.226

[15] A. Polyakov, V. Nikolaev, S. Stepanov, A. Almaev, A. Pechnikov, E. Yakimov, B.O. Kushnarev, I. Shchemerov, M. Scheglov, A. Chernykh, A. Vasilev, A. Kochkova, S.J. Pearton, J. Appl. Phys., **131** (21), 215701 (2022). DOI: 10.1063/5.0090832

[16] A.V. Almaev, B.O. Kushnarev, E.V. Chernikov, V.A. Novikov, P.M. Korusenko, S.N. Nesov, Superlatt. Microstruct., **151**, 106835 (2021). DOI: 10.1016/j.spmi.2021.106835